Vibrational Relaxation of Methane by Oxygen Collisions: Measurements of the Near-Resonant Energy Transfer between CH_4 and O_2 at Low Temperature

Corinne Boursier,* Joseph Ménard, and Françoise Ménard-Bourcin

Laboratoire de Physique Moléculaire pour l'Atmosphère et l'Astrophysique, UMR 1043, CNRS, Université Pierre et Marie Curie-Paris6, 4 place Jussieu, F-75005 Paris, France

Received: March 26, 2007; In Final Form: May 23, 2007

Vibrational relaxation in methane−oxygen mixtures has been investigated by means of a time-resolved pump−probe technique. Methane molecules are excited into selected rotational levels by tuning the pump laser to $2\nu_3$ lines. The time evolution in population of various vibrational levels after the pumping pulse is monitored by probing, near 3000 cm^{-1}, stretching transitions between various polyads like $2\nu_3(F_2) - \nu_3$, $(\nu_3+2\nu_4) - 2\nu_4$, and $(\nu_3+\nu_4) - \nu_4$ transitions. Measurements were performed from room temperature down to 190 K. A numerical kinetic model, taking into account the main collisional processes connecting energy levels up to 6000 cm^{-1}, has been developed to describe the vibrational relaxation. The model allows us to reproduce the observed signals and to determine rate coefficients of relaxation processes occurring upon CH_4-O_2 collisions. For the vibrational energy exchange, the rate coefficient of transfer from O_2 ($v = 1$) to CH_4 is found equal to $(1.32 \pm 0.09) \times 10^{-12}$ cm^3 $molecule^{-1}$ s^{-1} at 296 K and to $(1.50 \pm 0.08) \times 10^{-12}$ cm^3 $molecule^{-1}$ s^{-1} at 193 K.

I. Introduction

Collisional energy transfer in methane−oxygen mixtures has been the subject of numerous experimental and theoretical studies for nearly four decades. Concerning the specific near-resonant energy-transfer process between the dyad levels (near 1500 cm^{-1}) of CH_4 and the first vibrational level of O_2, the first measurement has been done by Yardley et al.[1] using the laser excited vibrational fluorescence technique at room temperature. There is no measurement of the rate coefficient of this transfer at lower temperatures. Concerning the process of vibration to translation energy transfer upon O_2 collisions, among various studies,[1−3] only the laser induced fluorescence measurements of Siddles et al.[3] were performed at low temperature.

A renewal of interest for the relaxation of methane by CH_4-O_2 collisions has appeared because of the evidence for non-thermal local equilibrium (non-LTE) in the terrestrial atmosphere.[4−8] Indeed, the knowledge of detailed vibrorotational relaxation of methane is essential for an accurate account or prediction of the infrared emission produced by a medium in non-LTE. Of course, for such applications, the relaxation of CH_4 must be investigated at low temperature.

The present paper is dedicated to the study of the relaxation of CH_4 in O_2 at room temperature and at 193 K. It is the continuation of previous works[9−12] concerning the vibrorotational energy-transfer processes implied in the relaxation of CH_4 after its excitation into a $2\nu_3(F_2)$ state by a pulsed laser radiation around 6000 cm^{-1}. In these previous studies, it has been shown that the time-resolved IR−IR double-resonance technique is particularly well adapted to this subject provided that numerous transitions are found in various vibrational bands. The kinetic model developed for describing relaxation in CH_4/N_2,[11] CH_4/H_2, or CH_4/He[12] mixtures has been modified to take into account the energy-transfer processes specific to the CH_4-O_2 collisions.

After a brief description of the experimental procedure in section II, experimental signals will be presented in section III. The analysis of the experiments by means of a kinetic model will be treated in section IV.

II. Experimental Technique

The experimental setup is very similar to that used in previous studies[9−12] and is described in detail in ref 12. Let us recall that CH_4 molecules are excited into a selected rovibrational level of the $2\nu_3(F_2)$ state by the single mode output beam of an Optical Parametric Oscillator (OPO) pumped by a single mode pulsed Nd:YAG laser (Continuum). The 7 ns output pulse produced by the signal wave near 1.66 μm (of about 5 mJ energy) has a spectral width of 0.02 cm^{-1}. The collision-induced time evolution of populations consecutive to laser excitation is monitored by the low-power beam of a cw single mode lead-salt diode laser (*Laser Photonics*) tunable in the 2939−2983 cm^{-1} range, which permits to probe various transitions of ν_3 harmonic and combination bands.

In order to investigate the relaxation of CH_4 excited to a selected rovibrational level of the $2\nu_3(F_2)$ state, various transitions have been probed: dyad−octad transitions, $(\nu_3+\nu_4) - \nu_4$ and $(\nu_3+\nu_2) - \nu_2$; pentad−tetradecad transitions, $2\nu_3 - \nu_3$ and $(\nu_3+2\nu_4) - 2\nu_4$; and tetradecad−triacontad transitions, $3\nu_3 - 2\nu_3$. A simplified diagram of the CH_4 vibrational levels with the main probed transitions is given in Figure 1. A more detailed description of the polyads of methane can be found in ref 13.

The pumping and probing beams propagate collinearly through the double-resonance cell, described in detail in ref 11, that is a variable temperature cell allowing measurements at low temperatures down to 190 K. It is a triple-walled Pyrex tube, 68 cm in length and 3.8 cm in internal diameter. The outer vacuum jacket is for thermal insulation, and the intermediate

* Corresponding author phone: +33 1 44274480; fax: +33 144277033; e-mail: boursier@ccr.jussieu.fr.

10.1021/jp072377y CCC: $37.00
Published on Web 07/04/2007

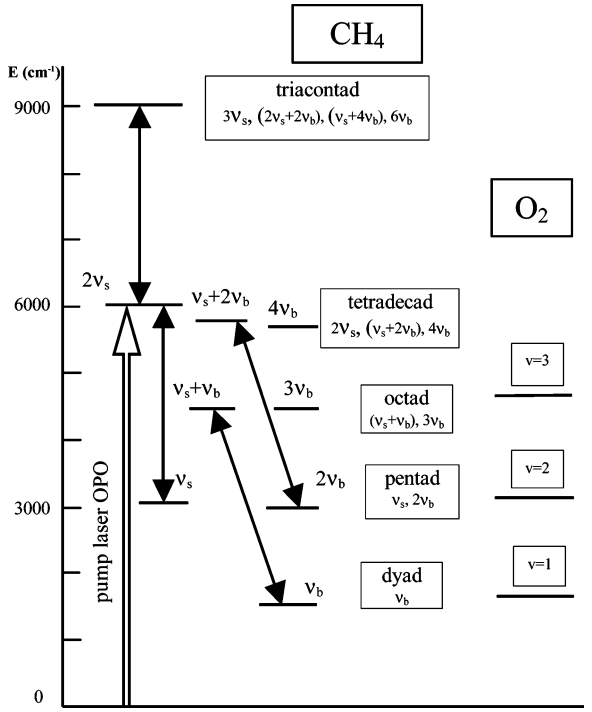

Figure 1. Simplified diagram of vibrational energy levels up to 9000 cm^{-1} showing the main transitions probed in this work. ≪ b ≫ is for bending and ≪ s ≫ is for stretching; $\nu_b = \nu_2$ or ν_4 and $\nu_s = \nu_1$ or ν_3.

one is for cooling the sample cell, which is obtained by flowing cold ethanol from a refrigerator (Maton) at a regulated temperature. The cell temperature is controlled by a chromel−alumel thermocouple placed in the cooling jacket. During the experiments, the temperature fluctuations did not exceed ±0.5 K.

Methane and oxygen were supplied by *Air Liquide* with a stated purity better than 99.998%. The gas pressures were measured using a MKS Baratron gauge for pressures up to 1 Torr (1 Torr=0.1333 kPa) and a Texas Instruments Bourdon gauge for the higher pressures.

Our measurements have been performed in CH_4/O_2 mixtures at 296 and 193 K for different gas pressures up to 82 hPa and by varying the methane molar fraction in the gas mixtures from 1% to 100%.

III. Experimental Results

A. Rotational Relaxation. As observed in CH_4/N_2 mixtures,[11] subsequent to the excitation of CH_4 molecules in a selected rotational level of the $2\nu_3(F_2)$ state, a fast equilibration of population occurs first in this state among the rotational levels of the same symmetry type as that of the laser-excited one, i.e., of the same nuclear spin modification. The total depopulation rate coefficients are measured by probing the laser-excited level. By pumping methane molecules into the $2\nu_3(F_2)$ $J = 1$, A_2, 18 level[14] via the R(0) line and by probing this level, depopulation rate coefficients upon CH_4-O_2 collisions were found equal to $(17.4 \pm 1.4)\ \mu s^{-1}\ Torr^{-1}$ or $(5.3 \pm 0.4) \times 10^{-10}\ cm^3\ molecule^{-1}\ s^{-1}$ at 296 K and $(21.6 \pm 1.5)\ \mu s^{-1}\ Torr^{-1}$ or $(4.3 \pm 0.3) \times 10^{-10}\ cm^3\ molecule^{-1}\ s^{-1}$ at 193 K. The value at 296 K is larger than that obtained for CH_4-N_2 collisions,[11] but the values at 193 K are very close to each other showing that oxygen like nitrogen is an efficient collision partner for depopulation of the rotational levels of methane in the excited vibrational state. Following the rotational relaxation, the vibrational energy-transfer processes that spread out energy from the $2\nu_3$ (F_2) state

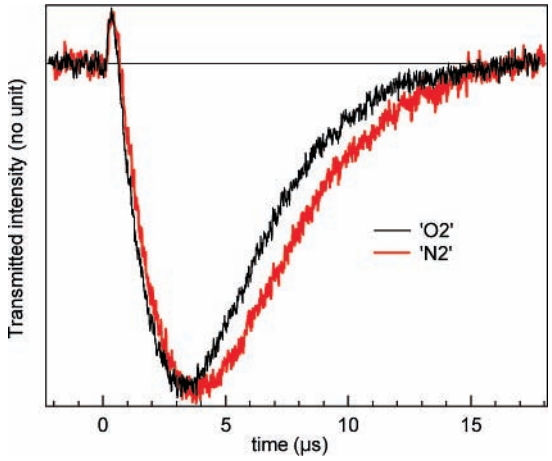

Figure 2. Comparison of experimental DR signals obtained by probing a $(\nu_3+2\nu_4) - 2\nu_4$ transition in a CH_4/O_2 or in a CH_4/N_2 mixture. For both signals the total pressure is 8 Torr, the molar fraction is 5%, and the temperature is 193 K.

to other vibrational states are slower than the rotational relaxation by about 1 order of magnitude.

B. Vibrational Relaxation. The vibrational relaxation is observed by monitoring the time evolution of the population of several vibrational states, from the dyad to the tetradecad, using well identified double-resonance (DR) signals corresponding to stretching transitions $\Delta v_3 = 1$.

The depopulation of the $2\nu_3$ vibrational state is well observed by probing a $2\nu_3(F_2) - \nu_3$ or a $3\nu_3 - 2\nu_3(F_2)$ transition for which the probed $2\nu_3$ rotational level is different from the laser-excited level. For these types of DR signals, no significant differences were observed between CH_4/N_2 and CH_4/O_2 mixtures as well as at room temperature at 193 K.

The major processes involved in the depopulation of the $2\nu_3$-(F_2) state are the intermode-energy-transfer processes that redistribute the vibrational energy within the polyad. They occur upon CH_4-CH_4 and CH_4-O_2 collisions. Indeed, our experimental data shows that the addition of oxygen to methane has the same effect as nitrogen to accelerate the equilibration of population within each polyad of interacting states. It can be deduced that the major processes involved in the depopulation of the $2\nu_3(F_2)$ state, namely the intermode processes, are as fast for O_2 collisions as for N_2 collisions.

The redistribution of vibrational energy within the tetradecad is also observable by probing a transition between a $2\nu_4$ level of the pentad and a $(\nu_3+2\nu_4)$ level of the tetradecad. DR signals obtained with such a probe are shown in Figure 2. The fast increase of population in $(\nu_3+2\nu_4)$ is observed in the way of a fast initial amplification. The amplified part of the IR double-resonance signals is weak. Indeed, the redistribution of molecules laser-excited in the $2\nu_3(F_2)$ state among all the states of the tetradecad is rapid due to the efficiency of intermode-transfer processes and leads to only a very small increase in population of the upper level of the probed transition. On the other hand, the lower level of the transition belongs to the $2\nu_4$ state that is the lower state of the pentad, and when the pentad states are equilibrated, the maximum of population is in this state. Thus the absorbed part of these signals is large. Indeed, by probing a $(\nu_3+2\nu_4) - 2\nu_4$ transition one observes mainly the time evolution of the population of the pentad state. The DR signals presented in Figure 2 were obtained at 193 K either in a CH_4/O_2 mixture or in a CH_4/N_2 mixture at 8 Torr total pressure with a methane molar fraction equal to 5%. As shown in this figure, the temporal evolution of this type of signal in CH_4/O_2 mixtures

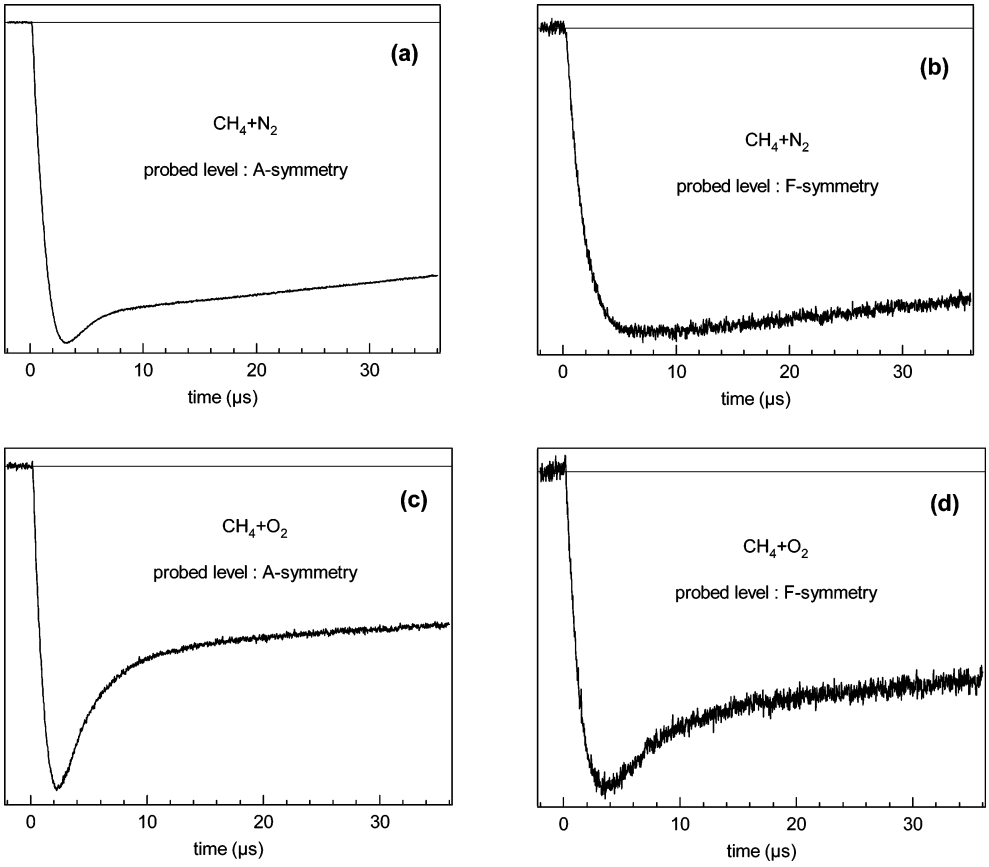

Figure 3. Comparison of experimental DR signals obtained in a CH_4/O_2 and in a CH_4/N_2 mixture by exciting into the $2\nu_3(F_2)$ $J = 1$, A_2, 18 level and probing $(\nu_3+\nu_4) - \nu_4$ transitions. For both mixtures the total pressure is 26 Torr, the molar fraction is 5%, and the temperature is 193K.

is different from what was previously observed in CH_4/N_2 mixtures. The DR signal obtained in the CH_4/O_2 mixture reaches its minimum earlier and returns more rapidly to equilibrium. That means that, as a result of O_2 collisions, the population of the pentad state reaches its maximum earlier and decreases more rapidly.

The difference between CH_4/O_2 and CH_4/N_2 mixtures is particularly striking for dyad states. The evolution of populations in the dyad is monitored by probing dyad−octad transitions. The same temporal behavior of the DR signals is observed for $(\nu_4+\nu_3) - \nu_4$ and $(\nu_2+\nu_3) - \nu_2$ transitions, but the DR signals depend on the symmetry type (A, E, or F) of the probed transition relative to the spin modification of the methane molecules excited by the pumping pulse.

In our experiments, methane molecules are excited onto a level of A-symmetry type. DR signals observed by probing an A-symmetry level and an F-symmetry level may be compared in Figure 3. These signals were obtained at 193 K in mixtures with a 5% methane molar fraction in 26 Torr total pressure.

The signals of Figure 3(a),(b) were obtained in a CH_4/N_2 mixture and these of Figure 3(c),(d) in a CH_4/O_2 mixture. As shown, the increase in population of A-symmetry levels of the dyad is faster than that of the other symmetry levels, and one observes a transient excess in populations of the A-symmetry levels compared to the levels of F-symmetry. This excess is due to the conservation of the spin modification in collisional processes. Indeed, the dyad levels become populated either by V−T transfer processes (loss of a bending quantum) or by near resonant V−V transfer processes. In the case of CH_4/N_2 mixtures the later processes occur only by self-collisions and involve the exchange of a ν_4 vibrational quantum between two methane molecules. Consequently, the filling of the F-symmetry levels is due to the promotion of molecules from the ground state, whereas the filling of the A-symmetry levels is due both to the promotion from the ground state and to V−T de-excitation from the upper A-symmetry levels. This temporary excess disappears by vibrational exchange (or swap) between methane molecules respectively on the dyad and ground states until an equilibrium is obtained in the distribution of the molecules in the various modifications of spin. Then all the dyad states return to Boltzmann equilibrium by V−T transfer processes, and the decrease in absorption of the signals proceeds at the same rate for all dyad−octad probes.

The rate coefficients of the near resonant V−V energy-transfer processes, involving the exchange of one quantum between two CH_4 molecules, have been determined in previous work[11] as also the rate coefficients of V−T de-excitation in N_2 collisions and self-collisions. The V−T processes are much slower than the V−V processes so that the main processes involved in the filling of the pentad and dyad states of methane in CH_4/N_2 mixtures remain essentially near-resonant V−V energy-transfer processes upon self-collisions even for CH_4 molar fractions as weak as 0.01% at 193 K.

The situation is totally different for CH_4 diluted in O_2, as the energy of the first vibrationally excited state of O_2 is close to the energy of the dyad levels of CH_4 so that near-resonant V−V transfer can occur.

By comparing DR signals obtained with a dyad−octad probe in CH_4/O_2 and CH_4/N_2 mixtures in the same conditions, the effect of O_2 collisions can be well observed. It can be seen in Figure 3 that for both symmetry species the signals reach their minimum earlier, and the increasing part of the DR signal corresponding to F-symmetry is very different. It shows that before the slow return to equilibrium of the dyad levels there is

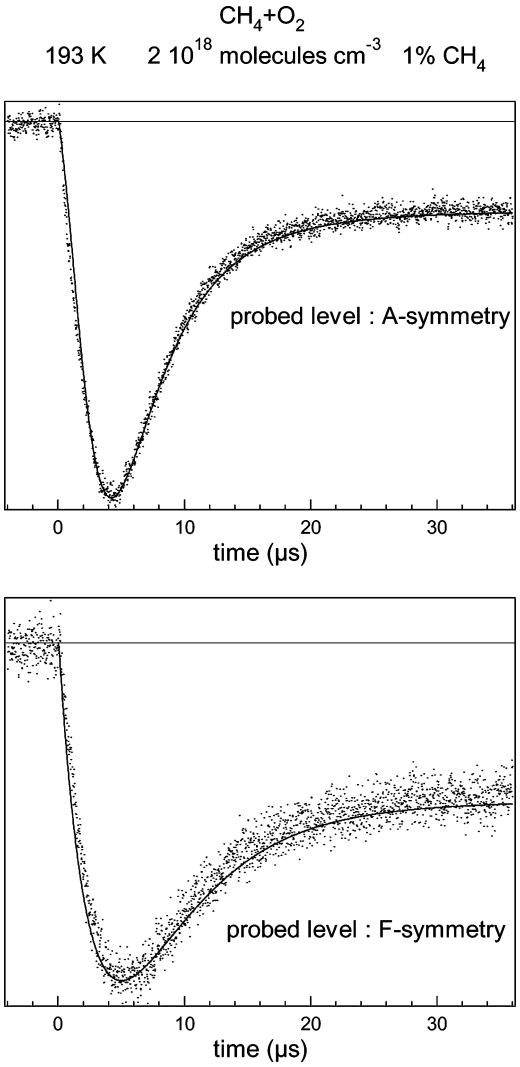

Figure 4. DR signals (dots) obtained at 193 K by probing dyad−octad transitions in a CH_4/O_2 mixture with a 1% methane molar fraction. The total pressure is 40 Torr (2×10^{18} molecules/cm^3). The simulated DR signals (line) are superimposed.

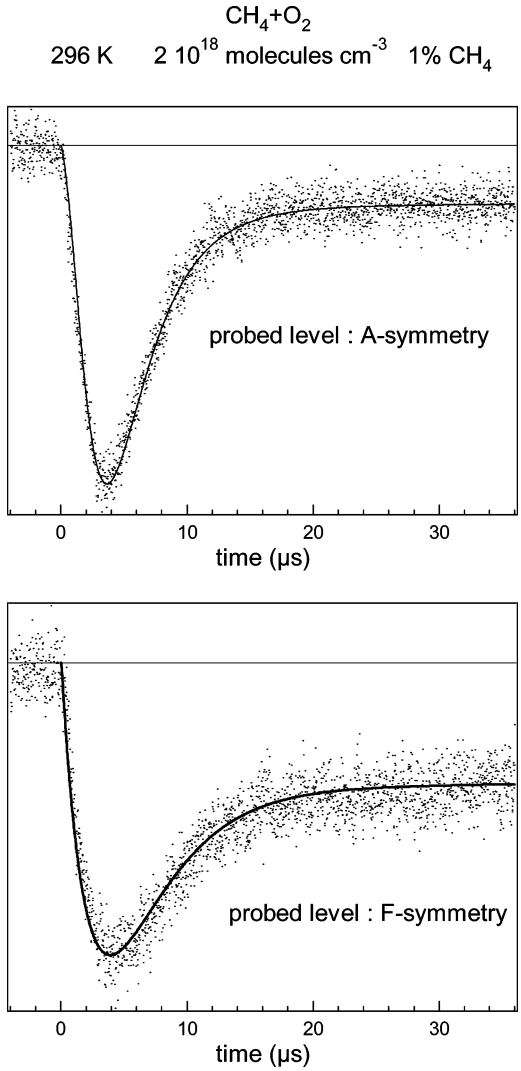

Figure 5. DR signals (dots) obtained at 296 K by probing dyad−octad transitions in the same gas sample as in Figure 4 (2×10^{18} molecules/cm^3). The simulated DR signals (line) are superimposed.

a faster decrease in population corresponding to V−V transfer between CH_4 and O_2 molecules.

It is particularly interesting to compare the temporal evolution of these DR signals as a function of the methane molar fraction and of the O_2 gas pressure for it allows determination of the part played by near-resonant V−V energy-transfer processes between CH_4 and O_2 molecules in filling lower polyads. For weak CH_4 molar fractions, the transfer to the lower polyads occurs predominantly via the resonant process, and, at each relaxation step, the energy released by CH_4 is transferred to oxygen molecules.

The effect of the temperature on the transfer processes between CH_4 and O_2 can be observed by comparing DR signals obtained in the same CH_4/O_2 mixture. Such signals obtained by probing dyad−octad transitions in a sample with 2×10^{18} molecules cm^{-3} and a 1% methane molar fraction are shown in Figures 4 and 5, at 193 K and at room temperature, respectively. It appears that the V−V energy transfer from excited CH_4 to O_2 is faster at 296 K than at 193 K, the number of molecules being constant. This behavior is contrary to that observed for V−V energy transfer between methane molecules.

IV. Analysis

A. Relaxation Processes. In order to obtain the rate constant of these processes we have modified the kinetic model developed for describing relaxation in CH_4/N_2[11] to take into account the energy-transfer processes specific to the CH_4-O_2 collisions. Due to the complexity of the energy levels of methane and because the molecules are excited rather high in energy (6000 cm^{-1}), only the vibrational aspect of the relaxation is described in the kinetic model. This model involves 90 states from the ground state to the tetradecad: 30 vibrational energy states and, for each of them, 3 overall rovibrational symmetry species C = A, E, or F (related to the total nuclear spin).

In the following, processes previously taken into account in the kinetic model are recalled, and processes specific to CH_4-O_2 collisions are presented.

(a) Intermode-Energy-Transfer Processes. These processes that redistribute the vibrational energy within a polyad can occur upon self-collisions as well as CH_4-O_2 collisions. In such collisions the symmetry type of the CH_4 molecules remains unchanged so that if one excites only one symmetry species, then the population of the rovibrational states of different symmetry is not affected by these processes. Three types are considered: transfer between stretching modes $\nu_3 \leftrightarrow \nu_1$, transfer

TABLE 1: Rate Coefficients for Intermode-Transfer Processes and V−V Transfer Processes in the ν_3 Mode

	rate coefficient (cm^3 $molecule^{-1}$ s^{-1})		rate coefficient (s^{-1} $Torr^{-1}$)	
processes	296 K[a]	193 K[a]	296 K[a]	193 K[a]
$CH_4(\nu_3,C) + CH_4 \rightarrow CH_4(\nu_2+\nu_4,C) + CH_4$	$(4.6 \pm 0.6) \times 10^{-11}$	$(3.6 \pm 0.4) \times 10^{-11}$	$(1.5 \pm 0.2) \times 10^{6}$	$(1.8 \pm 0.2) \times 10^{6}$
$CH_4(\nu_3,C) + O_2 \rightarrow CH_4(\nu_2+\nu_4,C) + O_2$	$(3.53 \pm 0.46) \times 10^{-11}$	$(2.8 \pm 0.4) \times 10^{-11}$	$(1.15 \pm 0.15) \times 10^{6}$	$(1.4 \pm 0.2) \times 10^{6}$
$CH_4(\nu_3,C) + CH_4 \rightarrow CH_4(\nu_1,C) + CH_4$	$(3.37 \pm 0.92) \times 10^{-11}$	$(2.6 \pm 0.8) \times 10^{-11}$	$(1.1 \pm 0.3) \times 10^{6}$	$(1.3 \pm 0.4) \times 10^{6}$
$CH_4(\nu_3,C) + O_2 \rightarrow CH_4(\nu_1,C) + O_2$	$(2.45 \pm 0.92) \times 10^{-11}$	$(1.8 \pm 0.5) \times 10^{-11}$	$(0.8 \pm 0.3) \times 10^{6}$	$(0.90 \pm 0.25) \times 10^{6}$
$CH_4(\nu_2,C) + CH_4 \rightarrow CH_4(\nu_4,C) + CH_4$	$(6.75 \pm 1.53) \times 10^{-11}$	$(4.8 \pm 0.8) \times 10^{-11}$	$(2.2 \pm 0.5) \times 10^{6}$	$(2.4 \pm 0.4) \times 10^{6}$
$CH_4(\nu_2,C) + O_2 \rightarrow CH_4(\nu_4,C) + O_2$	$>3.68 \times 10^{-11}$	$>2.8 \times 10^{-11}$	$>1.2 \times 10^{6}$	$>1.4 \times 10^{6}$
$CH_4(\nu_3,C) + CH_4(0, C') \rightarrow CH_4(0,C) + CH_4(\nu_3,C')$	$(2.45 \pm 0.92) \times 10^{-12}$	$(0.28 \pm 0.08) \times 10^{-11}$	$(0.8 \pm 0.3) \times 10^{5}$	$(1.4 \pm 0.4) \times 10^{5}$

[a] Temperature.

TABLE 2: Rate Coefficients for V−T Transfer Processes and V−V Transfer Processes in the ν_4 Mode

	rate coefficient (cm^3 $molecule^{-1}$ s^{-1})		rate coefficient (s^{-1} $Torr^{-1}$)	
processes	296 K[a]	193 K[a]	296 K[a]	193 K[a]
		VT CH_4		
$CH_4(\nu_4,C) + CH_4 \rightarrow CH_4(0,C) + CH_4$	$(3.2 \pm 0.5) \times 10^{-14}$	$(1.2 \pm 0.4) \times 10^{-14}$	$(1.05 \pm 0.15) \times 10^{3}$	600 ± 200
$CH_4(\nu_2,C) + CH_4 \rightarrow CH_4(0,C) + CH_4$	$(3.2 \pm 0.5) \times 10^{-14}$	$(1.2 \pm 0.4) \times 10^{-14}$	$(1.05 \pm 0.15) \times 10^{3}$	600 ± 200
		VT O_2		
$CH_4(\nu_4,C) + O_2 \rightarrow CH_4(0,C) + O_2$	$(5.7 \pm 1.4) \times 10^{-15}$	$(2.4 \pm 0.8) \times 10^{-15}$	(185 ± 45)	(120 ± 40)
$CH_4(\nu_2,C) + O_2 \rightarrow CH_4(0,C) + O_2$	$(5.7 \pm 1.4) \times 10^{-15}$	$(2.4 \pm 0.8) \times 10^{-15}$	(185 ± 45)	(120 ± 40)
		V−V CH_4		
$CH_4(\nu_4,C) + CH_4(0,C') \rightarrow CH_4(0,C) + CH_4(\nu_4,C')$	$(1.10 \pm 0.06) \times 10^{-11}$	$(1.16 \pm 0.06) \times 10^{-11}$	$(0.36 \pm 0.02) \times 10^{6}$	$(0.58 \pm 0.03) \times 10^{6}$
$CH_4(2\nu_4,C) + CH_4(0,C') \rightarrow CH_4(\nu_4,C) + CH_4(\nu_4,C')$	$(2.21 \pm 0.12) \times 10^{-11}$	$(2.32 \pm 0.12) \times 10^{-11}$	$(0.72 \pm 0.04) \times 10^{6}$	$(1.16 \pm 0.06) \times 10^{6}$
$CH_4(3\nu_4,C) + CH_4(0,C') \rightarrow CH_4(2\nu_4,C) + CH_4(\nu_4,C')$	$(3.31 \pm 0.18) \times 10^{-11}$	$(3.48 \pm 0.18) \times 10^{-11}$	$(1.08 \pm 0.06) \times 10^{6}$	$(1.74 \pm 0.09) \times 10^{6}$
$CH_4(4\nu_4,C) + CH_4(0,C') \rightarrow CH_4(3\nu_4,C) + CH_4(\nu_4,C')$	$(4.41 \pm 0.25) \times 10^{-11}$	$(4.64 \pm 0.24) \times 10^{-11}$	$(1.44 \pm 0.08) \times 10^{6}$	$(2.32 \pm 0.12) \times 10^{6}$
		V−V O_2		
$O_2(\upsilon=1) + CH_4(0,C) \rightarrow O_2(\upsilon=0) + CH_4(\nu_4,C)$	$(1.32 \pm 0.09) \times 10^{-12}$	$(1.50 \pm 0.08) \times 10^{-12}$	$(4.30 \pm 0.30) \times 10^{4}$	$(7.50 \pm 0.40) \times 10^{4}$
$CH_4(\nu_4,C) + O_2(\upsilon=0) \rightarrow CH_4(0,C) + O_2(\upsilon=1)$	$(1.33 \pm 0.09) \times 10^{-13}$	$(0.80 \pm 0.04) \times 10^{-13}$	$(4.34 \pm 0.30) \times 10^{3}$	$(4.00 \pm 0.20) \times 10^{3}$
$CH_4(2\nu_4,C) + O_2(\upsilon=0) \rightarrow CH_4(\nu_4,C) + O_2(\upsilon=1)$	$(2.66 \pm 0.19) \times 10^{-13}$	$(1.60 \pm 0.08) \times 10^{-13}$	$(8.68 \pm 0.60) \times 10^{3}$	$(8.00 \pm 0.40) \times 10^{3}$
$CH_4(3\nu_4,C) + O_2(\upsilon=0) \rightarrow CH_4(2\nu_4,C) + O_2(\upsilon=1)$	$(3.99 \pm 0.28) \times 10^{-13}$	$(2.40 \pm 0.12) \times 10^{-13}$	$(1.30 \pm 0.09) \times 10^{4}$	$(1.20 \pm 0.06) \times 10^{4}$
$CH_4(4\nu_4,C) + O_2(\upsilon=0) \rightarrow CH_4(3\nu_4,C) + O_2(\upsilon=1)$	$(5.32 \pm 0.37) \times 10^{-13}$	$(3.20 \pm 0.16) \times 10^{-13}$	$(1.74 \pm 0.12) \times 10^{4}$	$(1.60 \pm 0.08) \times 10^{4}$

[a] Temperature.

between bending modes $\nu_2 \leftrightarrow \nu_4$, and transfer between stretching and bending modes $\nu_3 \leftrightarrow (\nu_2+\nu_4)$.

(b) Near-Resonant Vibration−Vibration Energy-Transfer Processes between CH_4 Molecules. The most probable processes are the exchange of only one ν_3 or ν_4 quantum between two CH_4 molecules. These processes distribute the energy among the different polyads and contribute also to the distribution of vibrational excitation among the different symmetry species. Indeed, as the CH_4 molecules in the ground state may be in any symmetry type C = A, E, or F, when such a molecule encounters an excited one, it can be promoted either to ν_3 or ν_4 according to the process but conserves its symmetry type.

For the processes involving the exchange of one ν_3 quantum, we have considered the processes of vibrational swap between the ground state and ν_3

$$CH_4(\nu_3,C) + CH_4(0,C') \leftrightarrow CH_4(0,C) + CH_4(\nu_3,C') \quad (1)$$

with C≠C′ and the similar processes coupling the tetradecad to the pentad.

For the processes involving the exchange of one ν_4 quantum, we have considered the processes of vibrational swap between the ground state and ν_4

$$CH_4(\nu_4,C) + CH_4(0,C') \leftrightarrow CH_4(0,C) + CH_4(\nu_4,C') \quad (2)$$

and similar processes coupling the pentad to the dyad, the octad to the pentad, and the tetradecad to the octad.

(c) Near-Resonant Vibration−Vibration Energy-Transfer Processes between CH_4 and O_2. Contrary to the case of N_2 collisions that are not efficient in V−V transfer with CH_4 because of the large difference in energy of the vibrational quanta of these molecules, in O_2 collisions, these V−V transfer processes are efficient because the energy of the first vibrationally excited level of O_2 (1556.4 cm^{-1}) is very similar to the energy of the dyad levels of CH_4 (ν_2=1533.3 cm^{-1} and ν_4=1310.8 cm^{-1}). Actually, the probability of this type of transfer is linked not only to the small energy defect but also to the transition momentum. As the transition momentum is larger for ν_4 transitions, we consider only processes in which methane makes a ν_4 transition, while oxygen undergoes a $\Delta\upsilon = 1$ transition. It is worth noticing that the ν_2 and ν_4 states are strongly coupled, as mentioned above, and the ν_4 state is much more populated than the ν_2 state: 81.5% of the dyad population at 296 K and more than 88% at 193 K. The primary process

$$CH_4(\nu_4,C) + O_2(\upsilon = 0) \rightarrow CH_4(0,C) + O_2(\upsilon = 1) \quad (3)$$

contributes to relax energy from the dyad states of methane toward O_2 ($\upsilon = 1$).

The reverse process

$$CH_4(0,C) + O_2(\upsilon = 1) \rightarrow CH_4(\nu_4,C) + O_2(\upsilon = 0) \quad (3')$$

permits, as process 2, an equilibration among the levels of different symmetry types of methane because upon a collision with excited oxygen a methane molecule of any symmetry type may be excited to the dyad state.

At each relaxation step, the energy released by CH_4 is transferred to oxygen molecules. For example it is necessary to take into account, as for self-collisions, processes coupling the pentad to the dyad

$$CH_4(\nu_2+\nu_4,C) + O_2(\upsilon = 0) \rightarrow CH_4(\nu_2,C) + O_2(\upsilon = 1) \quad (4)$$

$$CH_4(2\nu_4) + O_2(\upsilon = 0) \rightarrow CH_4(\nu_4) + O_2(\upsilon = 1) \quad (5)$$

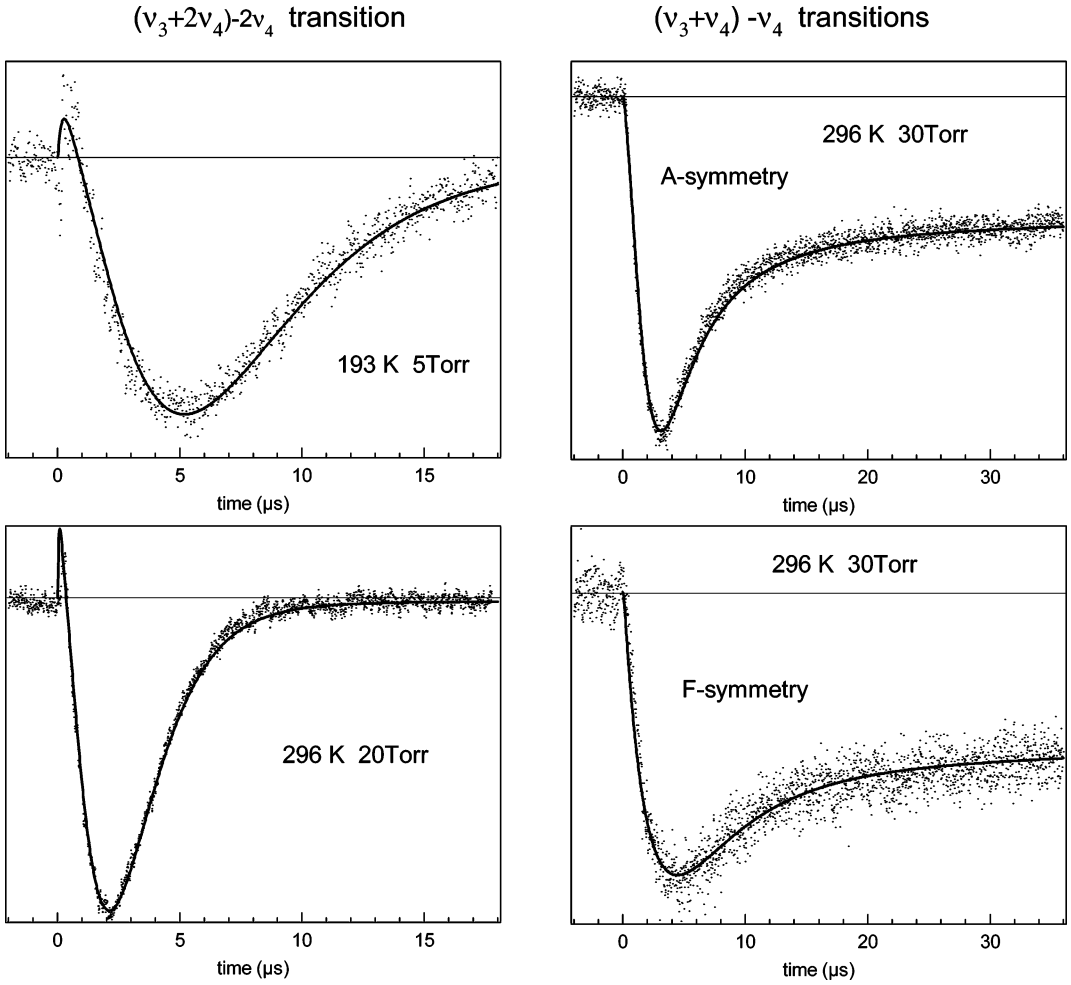

Figure 6. DR signals (dots) obtained in CH_4/O_2 mixtures with a 5% methane molar fraction by probing a $(\nu_3+2\nu_4)-2\nu_4$ transition or dyad−octad transitions after laser-excitation on an A-symmetry level of $2\nu_3(F_2)$. The simulated DR signals (line) are superimposed.

and processes coupling the octad to the pentad and the tetradecad to the octad.

These processes have been taken into account for all levels having at least one ν_4 quantum leading to 16 processes.

It has been suggested[1,2] that direct energy transfer from CH_4 (ν_3) to O_2 ($v = 2$) and processes of ladder-climbing in O_2 could play a small part in the relaxation of CH_4/O_2 mixtures. The first process that implies an exchange of two quanta of vibration between methane and oxygen was neglected in our model. Indeed, this exchange is less probable than the exchange of one quantum, and, due to the fast equilibration that occurs inside the pentad by intermode processes, the relaxation of molecules in the ν_3 state is more likely to happen through transfer to the $2\nu_4$ pentad state and then by energy transfer to O_2 according to the above process 5.

Concerning the ladder-climbing processes in oxygen, two processes were considered

$$O_2(v = 1) + O_2(v = 1) \rightarrow O_2(0) + O_2(v = 2) \qquad (6)$$

and

$$O_2(v = 1) + O_2(v = 2) \rightarrow O_2(0) + O_2(v = 3) \qquad (7)$$

(d) Vibration to Translation, Rotation (V-T,R) Energy-Transfer Processes. The V-T,R processes considered in our model involve the loss of one bending quantum. Such processes can occur upon self-collisions as well as CH_4-O_2 collisions, so, in the following processes, M will represent either a methane molecule or an oxygen molecule.

$$CH_4(\nu_4) + M \rightarrow CH_4(0) + M \qquad (8)$$

$$CH_4(\nu_2) + M \rightarrow CH_4(0) + M \qquad (9)$$

These processes have been taken into account for all levels having at least one bending quantum.

The V-T,R process of de-excitation of oxygen by collision with methane has also been introduced in our kinetic model:

$$O_2(v = 1) + CH_4 \rightarrow O_2(v = 0) + CH_4 \qquad (10)$$

The de-excitation of oxygen by itself was neglected, because, as outlined in ref 1, this process is particularly slow and the addition of a small amount of methane to oxygen enhances greatly the de-excitation of O_2.[15] Nevertheless, the rate coefficient of process 10 is expected[1] to vary between 1 and 10% of the rate coefficient of process 8.

(e) Simplifying Assumptions. For the same collision partner, all $\nu_3 \rightarrow \nu_1$ intermode-transfer processes considered in the exothermic direction ($\nu_3 > \nu_1$) have the same rate coefficient $k^M_{\nu 3 \rightarrow \nu 1}$ for M collisions (M=CH_4 or O_2). Similarly, for $\nu_2 \rightarrow \nu_4$ and for $\nu_3 \rightarrow \nu_2+\nu_4$ intermode-transfer processes, the rate coefficients of the exothermic processes have the same rate coefficients $k^M_{\nu 2 \rightarrow \nu 4}$ and $k^M_{\nu 3 \rightarrow \nu 2+\nu 4}$, respectively.

The rate coefficients of near-resonant V−V transfer processes between methane molecules are related by a scaling factor appropriate to first-order perturbation theory for harmonic oscillators. For instance, the rate coefficients for the processes

$$CH_4(n\nu_3, C) + CH_4(0) \rightarrow CH_4((n-1)\nu_3, C) + CH_4(\nu_3)$$

$$CH_4(n\nu_4, C) + CH_4(0) \rightarrow CH_4((n-1)\nu_4, C) + CH_4(\nu_4)$$

are n times the rate coefficient of processes 1 and 2, respectively.

The same assumption was adopted for V−V transfer processes from excited methane to oxygen molecules. Hence, the rate coefficient of the following process

$$CH_4(n\nu_4, C) + O_2(0) \rightarrow CH_4((n-1)\nu_4, C) + O_2(v = 1)$$

is n times that of process 3.

It is worth noticing that the direction of the collisional process chosen is really important when doing the assumption of harmonic factor. Indeed, although process 3 is well adapted to describe the relaxation of methane, the exothermic process is process 3′ whose rate coefficient, noted k_{V-O2}, is much larger than that of process 3 (by a factor of about 10 at 296 K and 18 at 193 K from the detailed balance). Furthermore, the energy defect and equilibrium constant change from processes 3−5. Consequently, whereas the rate coefficient of process 5 is twice the rate coefficient of process 3, the reverse rate coefficient of process 5 is not simply twice the rate coefficient of process 3′ but 1.39 and 1.42 times k_{V-O2} at 296 and 193 K, respectively.

Finally, by applying the above assumptions and the detailed balance, all the rate coefficients for V−V transfer processes are obtained from only three rate coefficients: those of processes 1, 2, and 3′.

The rate coefficients of V-T,R transfer processes are also related to each other according to the harmonic oscillator approximation, i.e., the rate coefficients (M=CH_4 or O_2) of the process

$$CH_4(n\nu_4) + M \rightarrow CH_4((n-1)\nu_4) + M$$

are n times those of process 8. Furthermore, the rate coefficients of processes 8 and 9 were supposed to be equal.

B. Results and Discussion. From the kinetic model, a system of coupled nonlinear differential equations is obtained. This system is solved by a Runge−Kutta method yielding the time-dependent populations of the 90 states of methane and 4 states of oxygen considered in the model. Then, simulated DR signals directly comparable with the experimental signals are generated from the time-dependent populations of methane.

The experimental and simulated DR signals were compared for CH_4/O_2 mixtures with various pressures and molar fraction at 193 and 296 K. The values of the rate coefficients leading to the best fit of our data are given in Tables 1 and 2. The results for self-collisions reported in these tables are from ref 11. The very good agreement between experimental DR signals and signals calculated using the values of Tables 1 and 2 is shown in Figures 4−6.

Let us discuss the values of the rate coefficients reported in Tables 1 and 2.

(a) Intermode-Transfer Processes. As mentioned in section III, the same rate of depopulation of the $2\nu_3$ state was found in CH_4/O_2 as in CH_4/N_2 mixtures. As the constants that play a major part in this depopulation are $k^{O2}_{\nu3\rightarrow\nu2+\nu4}$ and to a lesser extent $k^{O2}_{\nu3\rightarrow\nu1}$, these constants were assumed to be identical to those measured for N_2 collisions. For the $\nu_2 \leftrightarrow \nu_4$ intermode processes a minimal value of $k^{O2}_{\nu2\rightarrow\nu4}$ was determined under which the filling of the upper state of the $(\nu_3+2\nu_4) - 2\nu_4$ probed transition is not as fast as seen experimentally. Actually, decreasing $k^{O2}_{\nu2\rightarrow\nu4}$ results in a broadening of the amplified part and a shift in time of the absorbed part of the DR signal for a $(\nu_3+2\nu_4) - 2\nu_4$ transition. As no significant difference was observed in the first rise of the DR signals for this type of transition when N_2 is replaced by O_2, the same rate coefficients are assumed for N_2 as for O_2 collisions.

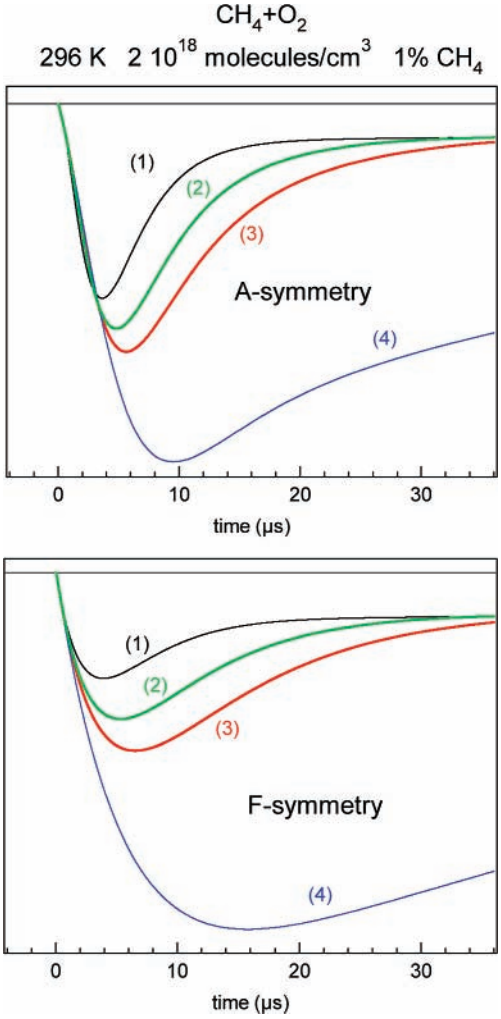

Figure 7. DR signals computed for dyad−octad transitions with different values of the rate coefficients of V−V energy transfer between CH_4 and O_2: signal (1), values of Tables 1 and 2 and signals (2−4), same as (1) except for the rate coefficient k_{V-O2} taken respectively at 2.4×10^4, 1.6×10^4, and 0 s^{-1} $Torr^{-1}$.

(b) V−V Energy Transfer in CH_4-O_2 Collisions. The shape of the signals simulated for dyad−octad probe transitions in CH_4/O_2 mixtures with small methane molar fraction, in particular the time position of the maximum of absorption of the signal (maximum of population in ν_4), was found to depend strongly on the processes of V−V energy transfer between CH_4 and O_2. This is illustrated in Figure 7 where computed DR signals have been plotted for A- and F-symmetry type $(\nu_3+\nu_4) - \nu_4$ transitions after laser excitation onto an A-symmetry type level. Signal (1) is obtained using the values of Tables 1 and 2, whereas for signals (2), (3), and (4) the rate coefficients of V−V energy transfer between CH_4 and O_2 were decreased by changing k_{V-O2} to 2.4×10^4 s^{-1} $Torr^{-1}$, 1.6×10^4 s^{-1} $Torr^{-1}$, and 0, respectively. Indeed, 2.4×10^4 s^{-1} $Torr^{-1}$ and 1.6×10^4 s^{-1} $Torr^{-1}$ are the values given in refs 1 and 2, respectively,

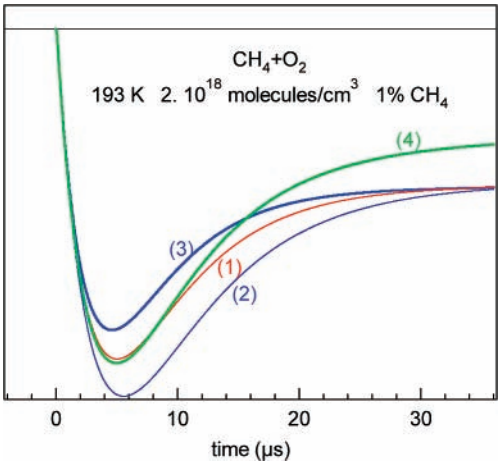

Figure 8. DR signals computed for an F-symmetry type dyad−octad transition with different values of the rate coefficients for CH_4-O_2 collisions: signal (1), values of Tables 1 and 2; signals (2) and (3), same as (1) except for the rate coefficients of V−V processes decreased by 20% and increased by 20%, respectively; and signal (4), same as (2) but the rate coefficients of V−T processes are multiplied by 5.

for the exothermic process 3′ at 296 K. It is clearly seen in Figure 7 that the efficiency of the energy transfer from oxygen to methane was underestimated in these previous works.

At 193 K, no comparison can be made with existing results, but the simulations presented in Figure 8 illustrate the way k_{V-O2} was determined in our experiments. In this figure, computed DR signals have been plotted for a F-symmetry $(\nu_3+\nu_4)-\nu_4$ probe transition after an A-symmetry type excitation. Signal (1) is obtained using the values of Table 1 and 2, whereas for signals (2) and (3) the value of k_{V-O2} has been changed from 7.5 to 6.0 × 10^4 s^{-1} $Torr^{-1}$ and 9.0 × 10^4 s^{-1} $Torr^{-1}$, respectively. For such rather small variations (±20%) of k_{V-O2} the shape of the signal changes rapidly. Furthermore, the shape of the initial signal (1) cannot be reproduced by taking a low value of k_{V-O2} (6.0 × 10^4 s^{-1} $Torr^{-1}$) and increasing the rate coefficient of the V−T transfer as shown in signal (4) of Figure 8.

A similar behavior, although less obvious, was observed for the maximum of absorption of the signals simulated for a $(\nu_3+2\nu_4)$-$2\nu_4$ probe and a small CH_4 molar fraction (between 1% and 10%). Since the values giving the best agreement for these two types of signals are consistent, we could obtain k_{V-O2} with a precision of about 10% at 193 K as well as 296 K.

For CH_4-CH_4 collisions, the V−V energy-transfer rate coefficients expressed in cm^3 $molecule^{-1}$ s^{-1} increase with decreasing temperature, but for the transfer from excited CH_4 to O_2, the rate coefficients decrease with decreasing temperature showing that these processes are not very resonant processes. For the temperature dependence of the rate coefficients for the reverse transfer (from excited O_2 to CH_4), contrary to the direct ones, they present a small increase with decreasing temperature when expressed in cm^3 $molecule^{-1}$ s^{-1} and a larger increase when expressed in s^{-1} $Torr^{-1}$.

(c) V−T Energy Transfer. The rate coefficients of these transfers are lower than those of V−V transfer between methane and oxygen. For V−T transfer processes, at room temperature, our results are in agreement with results of refs 1 and 16 for CH_4-O_2 collisions but higher than those of refs 2 and 3: (138 ± 7) and (101 ± 16) s^{-1} $Torr^{-1}$. At 193 K, our result for CH_4-O_2 collisions presents a larger discrepancy with the only available value[3] of (6 ± 1) 10^{-16} cm^3 $molecule^{-1}$ s^{-1} = (30 ± 5) s^{-1} $Torr^{-1}$. Let us notice that for such a small rate coefficient the determination is difficult and the accuracy worsens owing to beam flyout. These low values explain the slow increase of the dyad−octad signals. As de-excitation upon CH_4-O_2 collision by V−T processes is very slow, V−V processes play really a leading part in depletion of $2\nu_4$ levels and in the filling of ν_4 levels even for very small methane molar fractions.

In our model, we account for V−T de-excitation processes starting from all the excited levels having at least one quantum of bending assuming the same rate coefficient for ν_4 and ν_2. Indeed, it corresponds to a global rate coefficient for the de-excitation of the dyad with the same value as the individual rate coefficients presented in Table 1. Another way to model the de-excitation of the dyad is to neglect the V−T de-excitation from ν_2 and consequently to increase the rate coefficient of the V−T de-excitation from ν_4. Due to the ratio of populations into the ν_4 and ν_2 states, this alternative hypothesis would lead to 135 s^{-1} $Torr^{-1}$ at 193 K and 227 s^{-1} $Torr^{-1}$ at 296 K for the de-excitation of ν_4.

The V−T de-excitation of oxygen upon CH_4 collisions could not be obtained from the comparison of simulations with experimental results. No effect on the simulated DR signals for dyad−octad probes was observed by varying the rate coefficient of this process from 0 to 100% of the value found for the rate coefficient of the V−T de-excitation of methane upon O_2 collisions.

(d) Processes of Ladder-Climbing in Oxygen. The rate coefficient of these processes could not be measured from our experiments. These processes that allow a distribution of the energy among the vibrational energy levels of oxygen should be important when there is much energy in methane to transfer to oxygen. Simulations were carried out by varying the rate coefficient of processes 6 and 7 from 0 to the value of the rate coefficient of process 3′ that is an upper limit. We found that processes 6 and 7 are negligible in the experimental context of this work: excitation of methane molecules. When the methane molar fraction is small, simulations were done down to 5 ppmv, the ladder-climbing processes have no effect because there are plenty of O_2 molecules to absorb the energy from methane molecules. On the contrary, when the molar fraction is large (above 5%), relaxation through CH_4-CH_4 collisions becomes preponderant, and again the ladder-climbing processes in O_2 have no effect upon the DR signals we can observe.

V. Conclusion

The rate coefficient of the near-resonant transfer from methane to oxygen has been measured at room temperature and, for the first time, at a temperature low enough for applications to the terrestrial atmosphere.

The time-resolved double-resonance technique used in the present work is much more selective than the laser induced fluorescence or photoacoustic techniques used in previous studies.[1,2] With this technique, the time evolution of the population of well-defined vibrational levels was obtained directly from the experimental signals allowing us to measure the rate coefficient of the near-resonant transfer from methane to oxygen with a good accuracy.

Concerning the temperature dependence, the rate coefficient of the transfer from excited methane to O_2 (v = 1) remains about constant with decreasing temperature when expressed in s^{-1} $Torr^{-1}$ unit (and decreases slightly in cm^3 $molecule^{-1}$ s^{-1} unit), whereas the rate coefficient of the transfer from O_2 (v = 1) to methane increases with decreasing temperature for both units.

The kinetic model developed for CH_4-O_2 collisions has proved efficient to reproduce the DR signals obtained with various probes and various mixture conditions after laser-excitation in the $2\nu_3(F_2)$ vibrational state. It could be useful to predict, in circumstances not attainable in our experiments, the evolution of the population of methane and oxygen vibrational levels.

References and Notes

(1) Yardley, J. T.; Moore, C. B. *J. Chem. Phys.* **1968**, *48*, 14.
(2) Avramides, E.; Hunter, T. F. *Chem. Phys.* **1988**, *88*, 5506.
(3) Siddles, R. M.; Wilson, G. H.; Simpson, C. J. S. M. C*hem. Phys.* **1994**, *188*, 99.
(4) Lopez-Puertas, M.; Funke, B.; Gil-Lopez, S.; Lopez-Valverde, M. A.; von Clarmann, T.; Fischer, H.; Oelhaf, H.; Stiller, G.; Kaufmann, M.; Koukouli, M. E.; Flaud, J.-M. *C. R. Phys.* **2005**, *6*, 848.
(5) Lopez-Puertas, M.; Taylor, F. W. In *Non-LTE radiative transfer in the atmosphere*; Taylor, F. W., Ed.; Series on Atmospheric, Oceanic and Planetary Physics; World Scientific Publishing: River Edge, NJ, 2001; Vol. 3.
(6) Martin-Torres, F. J.; Lopez-Valverde, M. A.; Lopez-Puertas, M. *J. Atmos. Sol.-Terr. Phys.* **1998**, *60*, 1631.
(7) Lopez-Puertas, M.; Koukouli, M. E.; Funke, B.; Gil-Lopez, S.; Glatthor, N.; Grabowski, U.; von Clarmann, T.; Stiller, G. P. *Geophys. Res. Lett.* **2005**, *32*, L04805.
(8) Shved, G. M.; Gusev, O. A. *J. Atmos. Sol.-Terr. Phys.* **1997**, *59*, 2167.
(9) Menard-Bourcin, F.; Doyennette, L.; Menard, J.; Boursier, C. *J. Phys. Chem. A* **2000**, *10*, 1021.
(10) Menard-Bourcin, F.; Boursier, C.; Doyennette, L.; Menard, J. *J. Phys. Chem. A* **2001**, *105*, 11446.
(11) Boursier, C.; Menard, J.; Doyennette, L.; Menard-Bourcin, F. *J. Phys. Chem. A* **2003**, *107*, 5280.
(12) Menard-Bourcin, F.; Boursier, C.; Doyennette, L.; Menard, J. *J. Phys. Chem. A* **2005**, *109*, 3111.
(13) Boudon, V.; Rey, M.; Loete, M. *J. Quant. Spectrosc. Radiat. Transfer* **2006**, *98*, 394.
(14) The assigned quantum numbers *J*, *C*, and *N* represent the angular momentum, the rovibrational symmetry, and a running number according to increasing energies within the polyads, see: Champion, J.-P.; Loëte, M.; Pierre, G. In *Spectroscopy of the Earth's Atmosphere and Interstellar Medium*; Rao, K. N., Weber, A., Eds.; Academic Press: San Diego, CA, 1992; pp 339−422.
(15) Schnauss, U. E. *J. Acoust. Soc. Am.* **1965**, *37*, 1.
(16) Yardley, J. T.; Fertig, M. N.; Moore, C. B. *J. Chem. Phys.* **1970**, *52*, 1450.